The Oxford SWIFT integral field spectrograph

Niranjan Thatte[a], Matthias Tecza[a], Fraser Clarke[a], Timothy Goodsall[a], James Lynn[a], David Freeman[b] and Roger L. Davies[a]

[a]Dept. of Astrophysics, University of Oxford,DWB, Keble Road, Oxford, OX1 3RH, U.K.
[b]19 Sanderstead Court Avenue, South Croydon, Surrey CR2 9AU, U.K.

ABSTRACT

We present the design of the Oxford SWIFT integral field spectrograph, a dedicated I and z band instrument (0.65μm-1.0μm at R$\sim$4000), designed to be used in conjunction with the Palomar laser guide star adaptive optics system (PALAO, and its planned upgrade PALM-3000). It builds on two recent developments (i) the improved ability of second generation adaptive optics systems to correct for atmospheric turbulence at wavelengths $\leq 1\mu$m, and (ii) the availability of CCD array detectors with high quantum efficiency at very red wavelengths (close to the silicon band edge). Combining these with a state-of-the-art integral field unit design using an all-glass image slicer, SWIFT's design provides very high throughput and low scattered light.

SWIFT simultaneously provides spectra of $\sim$4000 spatial elements, arranged in a rectangular field-of-view of 44×89 pixels. It has three on-the-fly selectable pixel scales of $0\farcs24$, $0\farcs16$ and $0\farcs08$. First light is expected in spring 2008.

Keywords: integral field spectrograph, adaptive optics, image slicer, VPH grating, fully depleted CCD array detector

1. INTRODUCTION

The Oxford SWIFT integral field spectrograph is designed to exploit a particular scientific niche: observations in the wavelength range 800 nm – 1000 nm with an instrument at least twice as sensitive as any facility spectrograph in operation today. This will permit detailed studies of a large number of galaxies in the *redshift desert* – galaxies with $1 < z < 2$ that cannot presently be studied in detail as all prominent emission features are red-shifted out of the wavelength range of most optical spectrographs.

The development of SWIFT is timely – second generation adaptive optics systems, assisted by laser guide stars, are now capable of providing substantial improvement in ensquared energy in this wavelength range ([1], [2,3], [4]), although the achieved spatial resolution is still far from the diffraction limit. In addition to the factor of two gain in ensquared energy is a second gain in sensitivity that is at least as large. The latter stems from the development of $\sim$200 μm thick, fully depleted, large format CCD array detectors, that have very high quantum efficiency (and low fringing) at wavelengths close to the silicon band edge ([5], [6], [7]). SWIFT plans to be the first facility integral field spectrograph at a large telescope to incorporate these detector arrays with extreme red sensitivity.

SWIFT incorporates a novel design of an all-glass de-magnifying image slicer [8] that uses flat slicing and pupil mirrors combined with a lens mosaic to provide extremely high throughput ($\sim$95%), whilst maintaining very high surface quality leading to negligible scattered light even at these relatively short wavelengths. The superb performance of a classically polished all-glass image slicer with flat mirrors has already been demonstrated by the SPIFFI IFS ([9,10]), now part of the SINFONI instrument on the VLT [11,12]. In many ways, SWIFT complements near-infrared A.O. assisted integral field spectrographs like SINFONI at the VLT and NIFS at Gemini by extending the wavelength range to shorter wavelengths, where second generation A.O. systems can provide at least as good turbulence compensation. The night-sky OH emission lines that severely limit the sensitivity of most near-infrared spectrographs are much weaker in the I and z bands, providing a further sensitivity gain for SWIFT.

thatte@astro.ox.ac.uk, Tel: +44 1865 273412

Ground-based and Airborne Instrumentation for Astronomy, edited by Ian S. McLean, Masanori Iye,
Proc. of SPIE Vol. 6269, 62693L, (2006) · 0277-786X/06/$15 · doi: 10.1117/12.670859

Consequently, we expect SWIFT to provide a dramatic improvement in sensitivity compared to similar observations carried out at slightly longer wavelengths (slightly higher redshifts) in the J band. The sensitivity improvement enables a wide range of scientific programs to be carried out much more efficiently, indeed to be carried out at all. The salient ones are described in section 2. The detailed optical design of the instrument is presented in section 3, and the mechanics in section 4. SWIFT is to be installed as a facility instrument at the 200-inch Hale telescope at Palomar, together with the Palomar laser guide star assisted adaptive optics system PALAO ([13]). Caltech and JPL are jointly developing PALM-3000 ([3]), an upgrade to PALAO that will provide near diffraction limited performance over a large fraction of the SWIFT wavelength range. While PALM-3000 will not be available at SWIFT first light in spring 2008, the SWIFT design already incorporates enhancements that will allow it to exploit the improved performance delivered by PALM-3000.

The table below lists the key technical specifications of the Oxford SWIFT spectrograph.

Table 1. SWIFT technical specifications

Item	Specifications	
	minimum	optimal
Wavelength range	700 – 1000 nm	650 – 1000 nm
Spectral resolving power	3000	4000
Spaxel scales	0.″24, 0.″16	0.″24, 0.″16 & 0.″08
Number of spaxels	3900	4000
IFS spatial format	44 × 89	44 × 91
Operating temp. range	−10 to 25°C	−10 to 25°C
Field of view		
@0.″24/pixel	10.″3 × 20.″9	10.″3 × 21.″3
@0.″16/pixel	7.″0 × 14.″0	7.″0 × 14.″5
@0.″08/pixel	3.″5 × 7.″0	3.″5 × 7.″2

2. KEY SCIENCE PROGRAMS

Although SWIFT is designed to be a general purpose common user instrument, there are several key science programs where we expect SWIFT will make an impact. Three of these are briefly described below.

One of the highlights of SWIFT's scientific capabilities will be the study of galaxies, proto-galaxies, and their active nuclei at very high redshifts ($5 \leq z \leq 7$), through observations of the morphology, kinematics and dynamics of their Lyα emission, red-shifted into the SWIFT wavelength range. The recent discovery of QSOs at $z > 6$ by SDSS, with follow-up spectroscopic studies indicating that the epoch of reionization occurs at higher redshifts than previously expected, highlights the importance of studies in this redshift range. Furthermore, studying the kinematics of the large, spatially extended, Lyα haloes surrounding QSOs at high redshift will help establish the crucial connection between the visible and dark matter, thus providing constraints to theoretical models of structure formation in the early Universe.

Another area of research where SWIFT will excel is the measurement of dynamical masses of galaxies at moderate redshifts ($1 \leq z \leq 1.7$), in the range termed as the redshift desert. Although multi-object spectrographs at large telescopes also target this problem, the measurement of masses of galaxies that are spatially marginally resolved with a single long slit is fraught with peril. SWIFT data cubes, providing a complete 2D map of the kinematics at high spatial resolution, will lead to robust and secure mass estimates. These, in turn, will determine the evolution of the Tully-Fischer and Faber-Jackson relations with redshift.

The super-massive black holes thought to lurk in the nuclei of every galaxy in the local Universe form another topic where SWIFT can make an impact. Its unique combination of high sensitivity and good angular resolution will allow SWIFT to carry out a census of *stellar dynamical* mass determinations of super-massive black holes in nearby galaxies. Comparable instruments, working at infrared wavelengths, are limited to studying a few prototypical objects due to the higher night-sky background limiting their sensitivity.

3. OPTICS

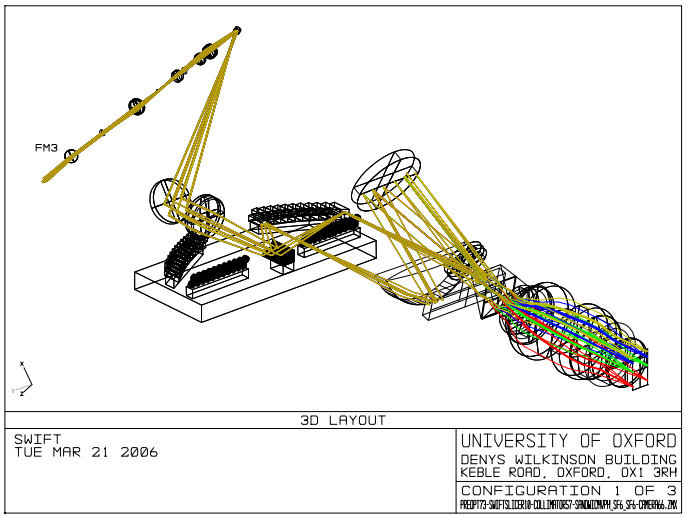

Figure 1. 3d layout of the SWIFT instrument. Only one of two spectrographs is shown. Light from the PALAO focus is picked up by fold mirror FM3 and folded into the pre-optics which is at an angle of $\approx 30^\circ$ to the SWIFT optical bench. After passing through the scale changer and anamorph focal reducer the light path is again folded with two mirrors before the field lens doublet images the PALMAO focal plane onto the slicer stack of the image slicer. After the image slicer the light from the two slicer exit slits is collimated by the spectrograph collimator, dispersed by the sandwiched VPH grating, and finally imaged onto the CCD detector by the spectrograph camera.

This section gives a summary of the entire SWIFT optical layout, listing first order optical parameters in Table 2 and showing the overall layout in Figure 1. The optics of SWIFT can be divided into three major modules: pre-optics, image slicer, and spectrograph, each of which comprises of several sub-systems. Each module re-images its input field, and the three modules are designed and optimised independently which in turn allows testing the modules indiviually before assembly. Details of each module and its sub-systems and analyses of them can be found in subsequent sections. Note that with the exception of two lenses that provide the required anamorphic magnification in the pre-optics, all surfaces are spherical, ensuring that they can be polished with classical techniques to achieve very high surface quality.

3.1. Pre-optics

The pre-optics module is responsible for imaging the AO focal plane onto the SWIFT image slicer with the required spaxel scale (or slice width). The largest pixel scale supported by the SWIFT image slicer is $0\farcs235$/pixel, which is a good match to the AO improved PSF. The image scale at the PALAO corrected focal plane is $2\farcs582$/mm or 387.3 μm $/\farcs1$. This image scale has to be magnified to match the correct image scale in the slicer focal plane of 0.47mm/$0\farcs235$ and 0.235mm/$0\farcs235$ across and along the slices, respectively. SWIFT is designed with three interchangeable spaxel scales: $0\farcs235$, $0\farcs16$, and $0\farcs08$, the last scale intended to be used with the very high order adaptive optics system PALM-3000, planned to be installed at the Palomar 200 inch.

While it is expected that PALM-3000 will not be available from the outset, it is necessary to include the design for the $0\farcs08$ spaxel scale from the very beginning in the design, as most likely it will not be possible to retro-fit the optics for the third image scale at a later stage, especially as the focal length and hence optical path length increases for the smaller spaxel scales.

The pre-optics design can be divided into two stages: the first stage relays the PALAO focal plane (and the telescope pupil, see Figure 2), the second stage relays this intermediate focal plane onto the slicer stack and re-images the telescope pupil to a distance 162mm beyond the slicer stack, so as to match the entrance pupil of the image slicer (see [8]). The first stage comprises a cemented doublet, which is different for each spaxel scale,

Table 2. SWIFT design specifications

Item	Specifications
Slice width	0.47 mm
Slit length	2 × 115.4 mm
Slit centers separation	230.0 mm
Input f-ratio	15.64
Anamorphic mag factor	2:1
Slicer input f-ratio	40.59 × 81.55
Slicer de-magnification	0.24
Collimator f-ratio	9.69 × 19.33
Camera f-ratio	2.49 × 6.32
Detector format	2 × 2048×4096
Slitlet format	2 × 22×89
Curvature of spectra	±0.9 pixels
Image quality	>80% ensq. energy in 1 pixel

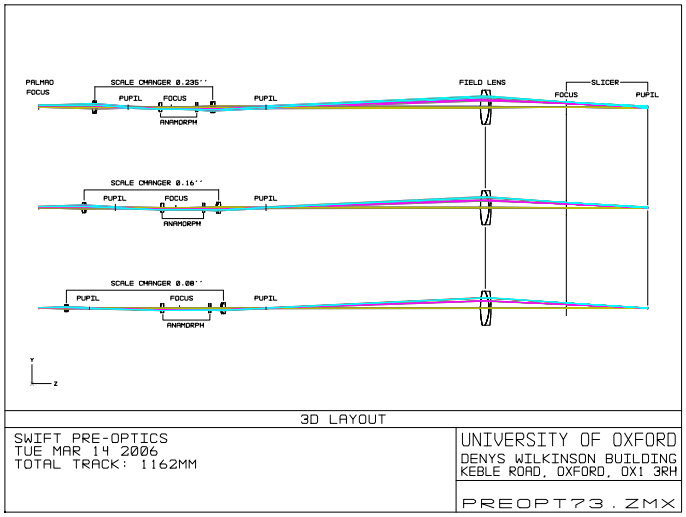

Figure 2. Layout of the pre-optics for all three spaxel scales: 0.″235 (top), 0.″16 (middle), 0.″08 (bottom).

and the second stage comprises a cemented doublet and a field lens doublet, which are identical for all spaxel scales. However, only the field lens doublet has the same location in all three scales and can be common to all scales. It is foreseen to manufacture three lenses of the cemented doublet and change the entire set of lenses prior to the field lens when changing scale (see also Figure 2).

The pre-optics includes, apart from the scale changer and a field lens, also an anamorphic focal reducer. The purpose of the anamorphic optics is to ensure proper Nyquist sampling of the slit along the spectral direction (i.e. a slit width of >2 pixels) while maximising the number of independent spectra simultaneously observed by a given detector. The scale changer provides the the correct magnification from the AO focal plane into the slicer focal plane along the slices, and the same magnification across the slices. The anamorphic focal reducer provides a ×1/2 anamorphic magnification along the slices. The anamorph focal reducer consists of two simple cylindrical lenses – one plano-convex and the other plano-concave. The plano-concave lens is the same for each scale but its location changes, the plano-convex is different for each scale. As with the scale changing optics it is foreseen to produce three lenses of the concave-plano cylindrical lens and change the entire set of pre-optics, except the field lens, when changing scale. Figure 2 shows the layout of the pre-optics for the three different

scales, without the fold mirrors necessary to pack the light path into the space envelope available for SWIFT (see section 4).

An important feature of this design is that the scale changer provides an intermediate pupil plane where we can place a pupil baffle. Depending on the chosen scale the pupil diameter will change accordingly. If we didn't have a pupil location where we can place a stop of appropriate size – and there is no pupil stop in the slicer or spectrograph (see section 3.3) – the stop size would be determined by the largest spaxel scale. At the smaller spaxel scales SWIFT would look past the nominal pupil, e.g. at the mount of the deformable mirror in PALAO, or perhaps even further at the telescope structure, depending on the chosen scale and the oversizing of the optics in SWIFT and/or PALAO. This pupil stop is therefore rather important, as it allows us to limit the background light entering SWIFT at all spaxel scales. The pre-optics also house the shutter and the order sorting filter in SWIFT.

3.2. Image Slicer

The SWIFT image slicer is a novel design that provides a compact exit slit geometry (demagnification of 0.24) whilst only using flat slicing and pupil mirrors. The advantage is that these can be classically polished to a very high quality surface finish, almost an order of magnitude better than typical diamond turned metal optics. The slicer uses a field lens before the slicer, and a lens mosaic after the slicer to achieve the desired focal plane demagnification and preserving the pupil. The all glass design is fabricated from Zerodur using optical contacting, providing high fill factor as well. The SWIFT slicer design and performance is discussed in detail in [8], so we do not present any details in this paper.

3.3. Spectrograph

The spectrograph module is responsible for dispersing the light from the slicer with the required spectral resolving power and imaging the spectra on to a detector. Two identical spectrographs are used, each taking the light from one of the two slicer exit slits as input. Each spectrograph consists of a collimator, a disperser, and a camera. Figure 3 shows a layout of the image slicer and one spectrograph.

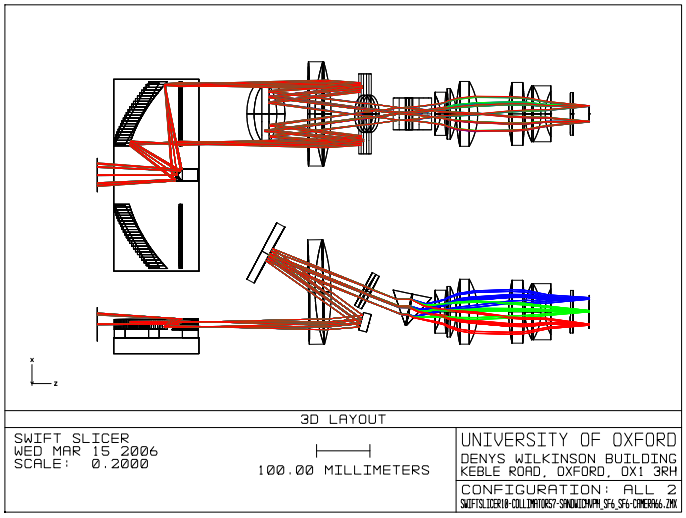

Figure 3. Layout of the slicer with one spectrograph. The pre-optics are not included in the view. The first collimator lens is shown full size, however, only the segment with the lower two thirds of the lens will be used, thus not obstructing the view from the fold mirror to the collimator mirror. Rays are shown for the inner- and outer-most slitlets and for three wavelengths, 650 nm (blue), 800 nm (green), and 1000 nm (red).

3.3.1. Collimator

Given the camera focal length, focal ratio, detector size, and slicer exit slit length the collimator is fully defined. The magnification of the spectrograph is $m = 0.266$. To achieve a compact layout we use a catadioptric design comprising of two cemented doublets and one concave, spherical mirror. Because of the off-axis design less than half of the full aperture is used. To make the spectrograph layout even more compact a fold mirror is inserted between the cemented doublets and the spherical mirror. Figure 4 shows the collimator layout without this additional fold, however, in Figure 3 the fold mirror is included. Because of distortion the effective focal length of the collimator is 438.714 mm, rather than the nominal value of 442.2 mm.

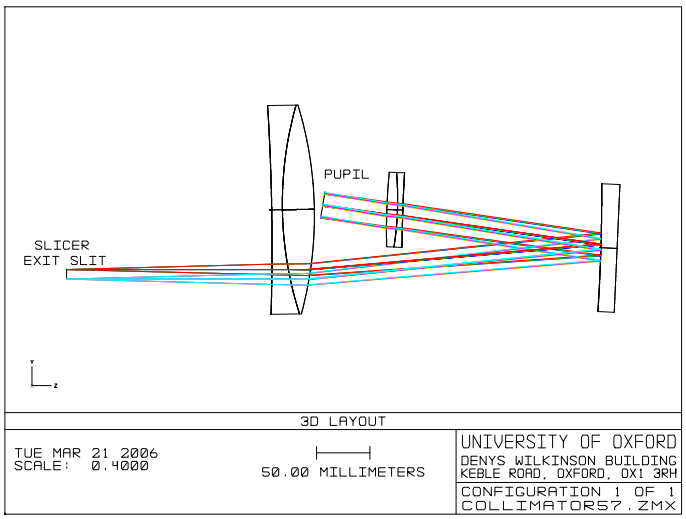

Figure 4. Layout of the SWIFT spectrograph collimator. The fold mirror is not in cluded in this view. Of the first doublet after the slicer exit slit only an off-axis segment will be used and the two doublets needed for SWIFT will be cut from one lens.

3.3.2. Sandwiched VPH grating

Volume phase holographic (VPH) gratings are especially attractive because of their high efficiency compared to ruled gratings, either directly ruled masters or replica gratings. However, they tend to have narrow diffraction peaks, especially at high line densities. Using a fixed format VPH grating in an instrument that has large instantaneous wavelength coverage can be quite challenging. In particular, the change of angular dispersion with diffraction angle and the effect of anamorphic magnification from the grating can cause problems, especially when the angular range of the spectrum is very large. The first leads to a $\Delta\lambda$ decreasing with wavelength, which in turn leads to an increased R at long wavelengths – and reduced R for short wavelengths – compared to the expected traditional behaviour of constant $\Delta\lambda$ for a grating spectrograph. The effect of anamorphic magnification means that the exit slit width is a function of wavelength and can be smaller than two detector pixels, effectively undersampling the spectrum.

To compensate for the increase of R with wavelength we investigated the combination of a VPH grating with a prism as a pre- and/or post-disperser. The refractive index of all optical glasses decreases with wavelength, hence a prism has higher dispersion at shorter wavelengths. This is opposite to a grating disperser and offers the potential to get a flat resolving power curve as a function of wavelength. An additional advantage of this configuration is a reduced line density of the VPH grating as the dispersive powers of prism and grating add. The advantage lies in the increased peak efficiency of the lower line density VPH grating.

From several layouts we finally chose a VPH grating sandwiched between two identical prisms. It has the advantage that it has the same number of air-glass interfaces as a simple VPH grating, provides enough deviation of the incident beam to allow a compact mechanical layout, and the spectral resolving power and exit slit width

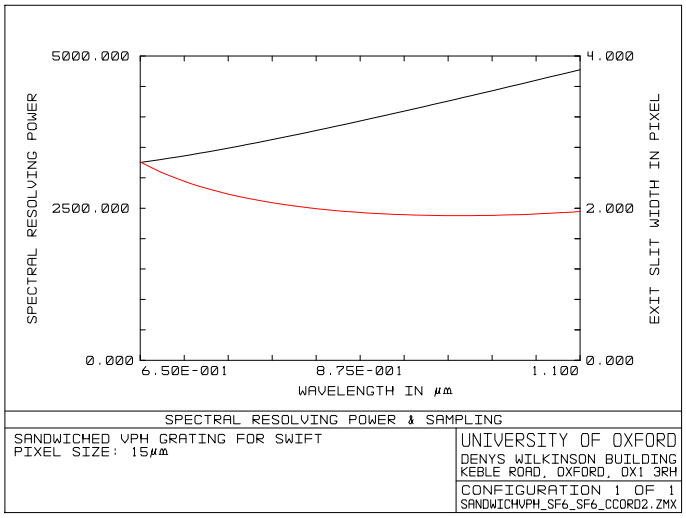

Figure 5. Spectral resolving power (black line) and exit slit width (red line) as a function of wavelength for a prism sandwiched VPH grating as used in the SWIFT spectrograph.

change far less with wavelength than a simple VPH grating (Figure 5). The prisms increase R at short wavelengths and decrease R at long wavelengths, thereby flattening the wavelength-v/s-R curve.

The anamorphic property of the grating leads to both slit and spectrum curvature. The slit curvature has no negative impact and is taken into account by the wavelength calibration. The spectrum curvature has two possible adverse effects on the data. Firstly, if the spectrum is tilted or curved it can be that the spectra at the edge of the slit are not fully imaged on to the detector. Secondly, to extract spectra along a curved trace requires resampling and interpolation which increases the noise in the data. Even though this is common practise in long-slit data reduction, controlling the curvature and tilt of the spectrum can greatly enhance the data quality and improve SWIFT's sensitivity. The deviation of a spectrum of a point source from a straight line has been controlled over the full length of the slit and is less than ± 0.9 detector pixels.

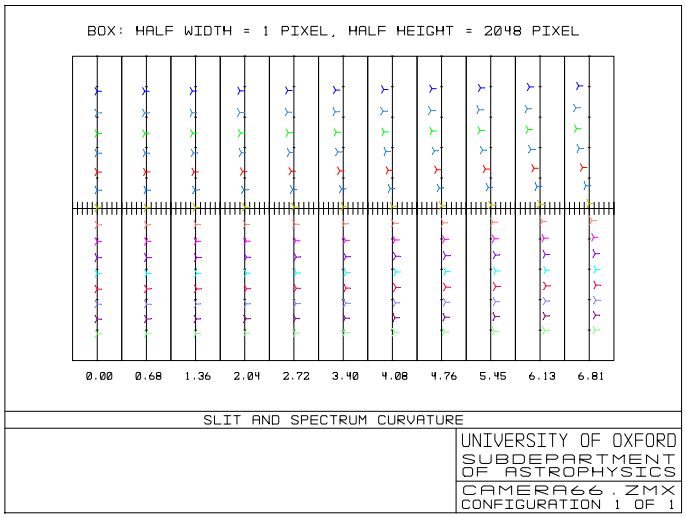

Figure 6. Spectrum and slit curvature of the SWIFT spectrograph camera. For eleven field positions along the half-slit we "trace" a spectrum at 15 discrete wavelengths. Shown is the deviation from the straight spectrum, the box for each spectrum is two detector pixels wide (30 μm) and 4096 detector pixels tall.

3.3.3. Camera

The minimum camera focal length, determined by the requirement to image the slit width on to two detector pixels, and by the grating size required to achieve the desired resolving power, is 114.4 mm. The camera images the dispersed spectrum on a 61.44 mm detector (4096 pixels of 15 μm). It is not possible to design a camera with just the minimum focal length, such a large field of view, and achieve an image quality exceeding the technical specification of 80% ensquared energy in one pixel. Instead, we chose a slightly longer camera focal length of 117.6 mm, leading to a collimated beam of size 45mm $\times$ 22.5 mm (elliptical). Figure 7 shows the layout of disperser and the camera. The total path length from the VPH to the detector is $\approx$ 400 mm.

The camera is setup and optimised together with the disperser, the window and the detector. The last two are parallel, but tilted to allow for axial colour. The lens is optimized at wavelengths 1000, 950, 900, 850, 801, 750, 700, and 650 nm. The 650nm wavelength is included in the optimisation but with a low weighting. The camera comprises of six elements, four single lenses and one cemented doublet closest to the detector, plus one cryostat window. Standard Schott glasses are used for the lenses, the window is made from fused silica.

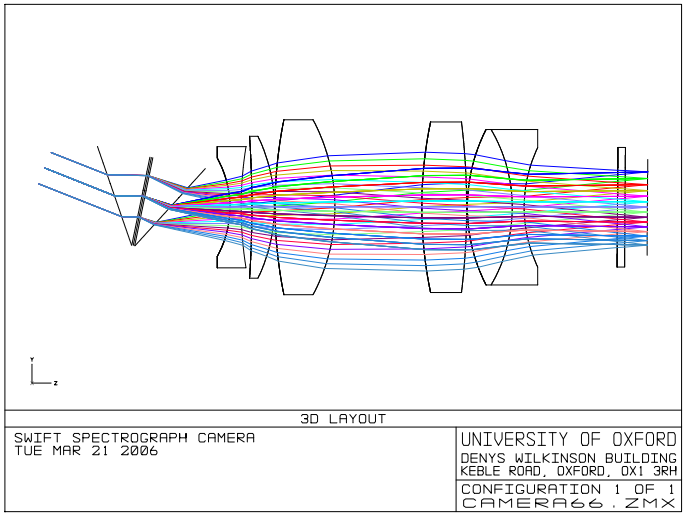

Figure 7. Layout of the SWIFT spectrograph camera shown together with the sandwiched VPH grating. The view is is a cut in the plane of dispersion showing 8 wavelengths from 650 nm to 1000 nm.

3.3.4. Detector

SWIFT will use two fully depleted, $\sim$200 μm thick, CCD detector arrys as its detectors, in a 2049 $\times$ 4096 format. These devices have impressive quantum efficiency, exceeding 80% at 950 nm, a gain of almost a factor of three over conventional deep depletion CCDs. The high Q.E. also leads to lower fringing, especially important in the I and z bands due to the large number of atmospheric OH emission lines present. At present, three manufacturers ([5–7]) are developing detectors satisfying the instrument requirements, a final choice of vendor will be made in the coming months. The detector plane is not orthogonal to the optical axis of the camera, but tipped by $\sim$1° along the dispersion direction.

To achieve higher sensitivity we disperse the spectrum over only about 3300 detector pixels, while still fulfilling the R specification. This has the additional advantage that it is possible to use an `e2v` fully depleted thick CCD with a 13.5 μm pixel pitch without sacrificing spectral coverage. These CCDs are currently in development and are one of the contenders for the SWIFT detectors. The smaller width of the `e2v` CCD means that only a total slitlength of $\approx$104 mm can be imaged, equivalent to 20 slitlets. In this case the two top and two bottom slitlets of the SWIFT field-of-view would need to be sacrificed. However, the sampling along the slitlet would be finer with spaxel scales of 0.″235 $\times$ 0.″216, 0.″16 $\times$ 0.″144, and 0.″08 $\times$ 0.″072. The field-of-view would be 40 $\times$ 89 spaxels.

4. MECHANICS

The overall mechanical layout of the SWIFT spectrograph is presented in figure 8. A custom drilled sandwiched breadboard, of the type commonly used in optical benches, forms a stiff base plate of SWIFT. All sub-assemblies are mounted directly to the base plate, with the exception of the pre-optics scale changer, which is mounted on a subsidiary base orthogonal to the main base plate. There are only four moving mechanisms in the entire spectrograph, one provides for the change of pixel scale, a second feeds in light from the calibration unit, the third inserts a mask in the input focal plane for instrument calibration, and the fourth controls the shutter. The mechanical design uses lens mounts that reference each lens position using the curved optical surfaces of the lenses.

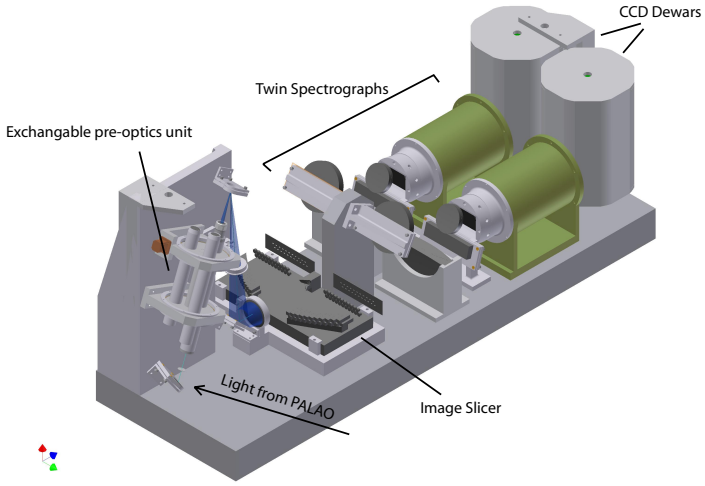

Figure 8. Overall mechanical layout of the Oxford SWIFT integral field spectrograph. The outer light-tight cover has been removed so as to reveal the opto-mechanical assembly.

4.1. Interface to PALAO

The SWIFT mechanical layout is subject to rather tight space constraints, as it has to be accomodated within the space available on the PALAO optical bench, and also allow the entire adaptive optics system (including SWIFT) to be lifted through the hatch in the Cassegrain cage and installed at the telescope. The latter operation is performed every time an instrument change at the Cassegrain focus is scheduled, typically once every fortnight. The total footprint of SWIFT is restricted to be 18 inches $\times$ 54 inches, the total height is to be no more than 26 inches. A very compact design and layout is required to meet these stringent constraints. As SWIFT is not the only back-end instrument for PALAO/PALM-3000, the mechanical interface also requires SWIFT to be easily removable and reproducibly re-mounted to the PALAO optical bench.

5. PERFORMANCE

Figure 9 shows the expected performance of the SWIFT spectrograph. The design utilises defocus as a means of balancing spherical aberration. This means that all the PSFs have unimpressive Strehl Ratios. Nevertheless, the FWHM of the diffraction PSF in the spatial direction is within 1 pixel at all wavelengths and all field points. Note that diffraction does have a significant effect and the performance predicted from the geometrical spot diagrams can be a bit misleading. Note that the 650 nm geometrical spot diagram extends to a height of about 2.5 pixels. Performance in the 700 to 1000 nm waveband seems to be worst at around 800/750nm due to secondary spectrum. For all wavelengths and field positions along the slit 80% of the energy is ensquared within a pixel of 12 μm , satisfying the requirement set out in the technical specifications.

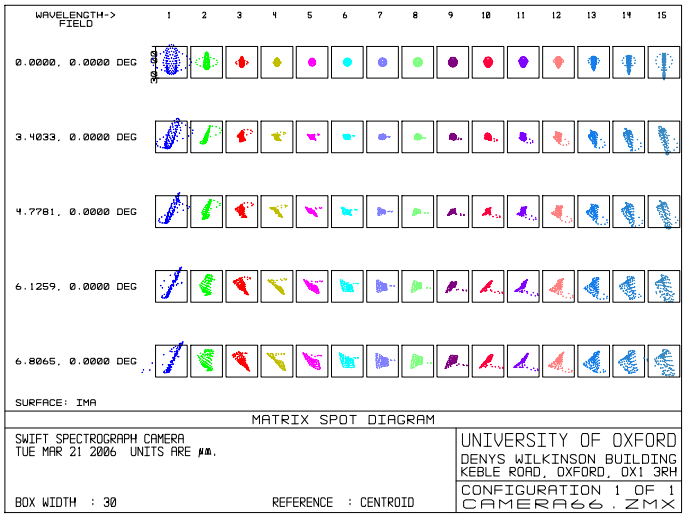

Figure 9. Spot diagrams showing the performance of the SWIFT spectrograph for five field points spanning the half slit and for 15 wavelengths. The box width corresponds to two detector pixels. Within each box, the dispersion direction is vertical, the spatial direction horizontal, contrary to what the matrix arrangement suggests.

The expected throughput of SWIFT is presented in table 3. We assume a 1% loss per air-glass surface, which should be practically achievable with anti-reflection coatings for the SWIFT wavelength range. The number of surfaces of each sub-system is given in parenthesis. Note that a minimum transmission of only 75% of the order sorting filter is a very conservative estimate.

Table 3. SWIFT throughput estimates

Component	Average throughput (%)	Peak throughput (%)	Minimum throughput (%)
Pre-optics (13)	87.8	87.8	87.8
order sorting filter	85.0	95.0	75.0
Slicer (4)	96.1	96.1	96.1
Collimator (6)	94.1	94.1	94.1
VPH grating (VPH+2)	83.3	93.1	63.7
Camera (12)	88.6	88.6	88.6
Total	**49.8**	**62.2**	**33.6**

In summary, the Oxford SWIFT spectrograph provides integral field spectroscopy of ∼4000 spaxels covering the wavelength range 650 – 1000 nm with very high throughput in a compact spectrograph design. It uses a novel image slicer design that utlises flat slicing optics made from glass, whilst maintaining a small slit length. Coupled with a second generation adaptive optics system and fully-depleted, ∼200 μm thick CCD array detectors, it provides high performance spectroscopy covering the I and z bands.

6. ACKNOWLEDGEMENTS

The Oxford SWIFT integral field spectrograph is directly supported by a Marie Curie Excellence Grant from the European Commission (MEXT-CT-2003-002792, Team Leader: N. Thatte). It is also supported by additional funds from the University of Oxford Physics Department and the John Fell OUP Research Fund. Additional

funds to host and support SWIFT at the 200-inch Hale Telescope on Palomar are provided by Caltech Optical Observatories.

REFERENCES

1. B. L. Ellerbroek, F. J. Rigaut, B. J. Bauman, C. Boyer, S. L. Browne, R. A. Buchroeder, J. W. Catone, P. Clark, C. d'Orgeville, D. T. Gavel, G. Herriot, M. R. Hunten, E. James, E. J. Kibblewhite, I. T. McKinnie, J. T. Murray, D. Rabaud, L. K. Saddlemyer, J. Sebag, J. Stillburn, J. M. Telle, and J.-P. Veran, "Multiconjugate adaptive optics for Gemini-South," in *Adaptive Optical System Technologies II. Edited by Wizinowich, Peter L.; Bonaccini, Domenico. Proceedings of the SPIE, Volume 4839, pp. 55-66 (2003).*, P. L. Wizinowich and D. Bonaccini, eds., pp. 55–66, Feb. 2003.
2. R. G. Dekany, M. Troy, G. Brack, C. A. Bleau, R. C. DuVarney, and M. A. Ealey, "1600 actuator tweeter mirror upgrade for the Palomar Adaptive Optics system (PALAO)," in *Proc. SPIE Vol. 4007, p. 175-179, Adaptive Optical Systems Technology, Peter L. Wizinowich; Ed.*, P. L. Wizinowich, ed., pp. 175–179, July 2000.
3. R. G. Dekany, A. H. Bouchez, M. C. Britton, and V. Velur, "PALM-3000: visible light AO on the 5.1-m Telescope,," in *Proc. SPIE Vol. 6272, paper 196, Advances in Adaptive Optics II, Brent L. Ellerbroek; Domenico Bonaccini; Eds.*, B. L. Ellerbroek and D. Bonaccini, eds., p. 196, 2006.
4. F. P. Wildi, G. Brusa, M. Lloyd-Hart, L. M. Close, and A. Riccardi, "First light of the 6.5-m MMT adaptive optics system," in *Astronomical Adaptive Optics Systems and Applications. Edited by Tyson, Robert K.; Lloyd-Hart, Michael. Proceedings of the SPIE, Volume 5169, pp. 17-25 (2003).*, R. K. Tyson and M. Lloyd-Hart, eds., pp. 17–25, Dec. 2003.
5. C. J. Bebek, K. S. Dawson, J. H. Emes, M. H. Fabricius, J. A. Fairfield, D. E. Groom, S. E. Holland, A. Karcher, W. F. Kolbe, N. P. Palaio, N. A. Roe, J. Saha, and G. Wang, "CCD development at Lawrence Berkeley National Laboratory," in *Proc. SPIE Vol. 6276, paper 12, High Energy, Optical, and Infrared Detectors for Astronomy II, David A. Dorn; Andrew D. Holland; Eds.*, D. A. Dorn and A. D. Holland, eds., p. 12, 2006.
6. P. R. Jorden, K. Ball, R. Bell, D. J. Burt, K. Hadfield, P. Jerram, P. J. Pool, A. Pike, A. D. Holland, and N. N. Murray, "Commercialization of full depletion scientific CCDs," in *Proc. SPIE Vol. 6276, paper 04, High Energy, Optical, and Infrared Detectors for Astronomy II, David A. Dorn; Andrew D. Holland; Eds.*, D. A. Dorn and A. D. Holland, eds., p. 04, 2006.
7. Y. Kamata, S. Miyazaki, H. Nakaya, E. Miyata, H. Tsunemi, T. G. Tsuru, S. Takagi, K. Miyaguchi, M. M., and H. Suzuki, "Recent results of the fully-depleted back-illuminated CCD developed by Hamamatsu,," in *Proc. SPIE Vol. 6276, paper 73, High Energy, Optical, and Infrared Detectors for Astronomy II, David A. Dorn; Andrew D. Holland; Eds.*, D. A. Dorn and A. D. Holland, eds., p. 73, 2006.
8. M. Tecza, N. Thatte, F. Clarke, T. Goodsall, and D. Freeman, "SWIFT image slicer: large format, compact, low scatter image slicing," in *Optomechanical Technologies for Astronomy. Edited by Atad-Ettedgui, Eli; Antebi, Joseph; Lemke, Dietrich. Proceedings of the SPIE, Volume 6273, paper 100 (2006).*, E. Atad-Ettedgui, J. Antebi, and D. Lemke, eds., p. 100, 2006.
9. M. Tecza, N. A. Thatte, F. Eisenhauer, S. Mengel, C. Roehrle, and K. Bickert, "SPIFFI image slicer: revival of image slicing with plane mirrors," in *Proc. SPIE Vol. 4008, p. 1344-1350, Optical and IR Telescope Instrumentation and Detectors, Masanori Iye; Alan F. Moorwood; Eds.*, M. Iye and A. F. Moorwood, eds., pp. 1344–1350, Aug. 2000.
10. M. Tecza, F. Eisenhauer, C. Iserlohe, N. A. Thatte, R. Abuter, C. Roehrle, and J. Schreiber, "SPIFFI Image Slicer: High-Precision Optics at Cryogenic Temperatures," in *Specialized Optical Developments in Astronomy. Edited by Atad-Ettedgui, Eli; D'Odorico, Sandro. Proceedings of the SPIE, Volume 4842, pp. 375-383 (2003).*, E. Atad-Ettedgui and S. D'Odorico, eds., pp. 375–383, Feb. 2003.
11. H. Bonnet, R. Abuter, A. Baker, W. Bornemann, A. Brown, R. Castillo, R. Conzelmann, and R. Damster, "First Light of SINFONI at the VLT," *The Messenger* **117**, pp. 17–+, Sept. 2004.

12. F. Eisenhauer, R. Abuter, K. Bickert, H. Bonnet, J. Brynnel, R. Conzelmann, B. Delabre, R. Donaldson, J. Farinato, E. Fedrigo, R. Genzel, C. Iserlohe, M. Kasper, C. Roehrle, J. Schreiber, M. Tecza, and N. Thatte, "SINFONI - Integral field spectroscopy at 50 milli-arcsecond resolution with the ESO VLT," in *Instrument Design and Performance for Optical/Infrared Ground-based Telescopes. Edited by Iye, Masanori; Moorwood, Alan F. M. Proceedings of the SPIE, Volume 4841, pp. 1548-1561 (2003).*, pp. 1548–1561, Mar. 2003.
13. M. Troy, R. G. Dekany, G. Brack, B. R. Oppenheimer, E. E. Bloemhof, T. Trinh, F. G. Dekens, F. Shi, T. L. Hayward, and B. Brandl, "Palomar adaptive optics project: status and performance," in *Proc. SPIE Vol. 4007, p. 31-40, Adaptive Optical Systems Technology, Peter L. Wizinowich; Ed.*, P. L. Wizinowich, ed., pp. 31–40, July 2000.